USD 544.225:546.27

K. Shirai (Osaka, Japan)

Electronic structures and mechanical properties of boron and boron-rich crystals (Part 2)

The second part of this review treats the phase diagram of boron, because of the importance of the material research. A comparison of the phase stabilities of related crystals has been made and deducing general trends among them has been attempted, from which the reader could get useful insights for future development of superhard materials. The mechanical properties of boron and boron-rich crystals are then discussed as the basis of superhard materials. This area is the primary source, from which many controversies arose regarding the strong intericosahedral bonding. Through working on many examples for deformation, consistent interpretations are given.

Key words*: boron-rich crystals, first-principles calculation, phase transition, mechanical properties.*

PHASE STABILITY

In the second part of this review, first we discuss the phase stability of boron at finite temperatures. This is a realm where free energy plays the central role. Phase diagram is the basic tool for material research. Without this it is difficult to search for new phases.

Phase diagram of boron

Since the discovery of the superconductivity for β-rhombohedral boron at p = 160 GPa, a big issue of this material is what is the structure around the superconducting transition. Sanz et al. found a structural transition to an amorphous phase at p > 100 GPa at room temperature [1]. They reported also that another rhombohedral structure appeared at p > 20 GPa under nonhydrostatic conditions. Ma et al. found a transition to a tetragonal phase at p > 10 GPa and T > 1500 K [2]. Theoretically, an α-Ga type structure was suggested [3—5]. There is no consensus about the structure when superconductivity takes place.

When the author started a study on this issue, he was surprised to see that there was no phase diagram for boron. Although α-rhombohedral boron is obtained commonly at relatively low temperatures [6], it was widely believed that β-rhombohedral boron is the most stable phase over all the temperatures of solid states. Probably, this believe comes from an authoritative reference of Hoard and Hughes [7]. Although they notice the fact of low-temperature synthesis of α-rhombohedral boron, it seems reasonable for them to consider that α-rhombohedral phase can be obtained only in some specific circumstances, for example, using specific starting materials. However, Kimura's group showed that, by starting from amorphous boron, α phase was obtained at a very narrow range of temperature around 1200 °C with the width ~ 20 degree [8]. Below this temperature, no crystallization occurred. Crystals of α phase were first isolated by molten metal,

where the eutectic temperature was as low as 830 °C for the B—Pt system [9] and similarly for the Pd—B system [10]. In the molten metal synthesis, the growth process is close to thermodynamic equilibrium. From these observations, it is most likely that α phase is the stable phase at low temperatures; otherwise it is difficult to understand low temperature synthesis of α-rhombohedral boron.

Before the author's study, DFT calculations about phase stability of boron were made only on simple hypothetical model structures, besides α-rhombohedral boron [13]. However, as seen from the precedent arguments, the comparison with β-rhombohedral boron is of crucial importance. The author performed DFT calculations with this motivation. After completing the total-energy calculations, along with other thermodynamic quantities, we found that α-rhombohedral boron is truly the ground state of boron, while β-rhombohedral boron is stable only at high temperatures [14]. The transition temperature is calculated to be about 1000 K at $p = 0$. The mechanism underlying this difference is rather simple; stiff materials are stable at low T, while soft materials can be stable at high T because of the entropic contribution of phonons. The situation is very like the situation of the diamond—graphite system. It is a common observation that a dense and thereby stiff phase (diamond) is stable at low T and at high p, while a dilute and thereby soft phase (graphite) is stable at high T and low p.

Based on the ground-state energy calculations along with phonon calculations, we predicted a phase diagram of boron for the first time [11]. This is shown in Fig. 1, *a*. Anharmonic effects are taken into account within quasiharmonic approximation. The phases, which are taken into consideration, are limited to α- and β-rhombohedral boron. Although there are still other polymorphs, these two are the extrema of boron modifications in many respects. We may think that other phases, if present in the phase diagram, can be placed in an intermediate region according to the stiffness.

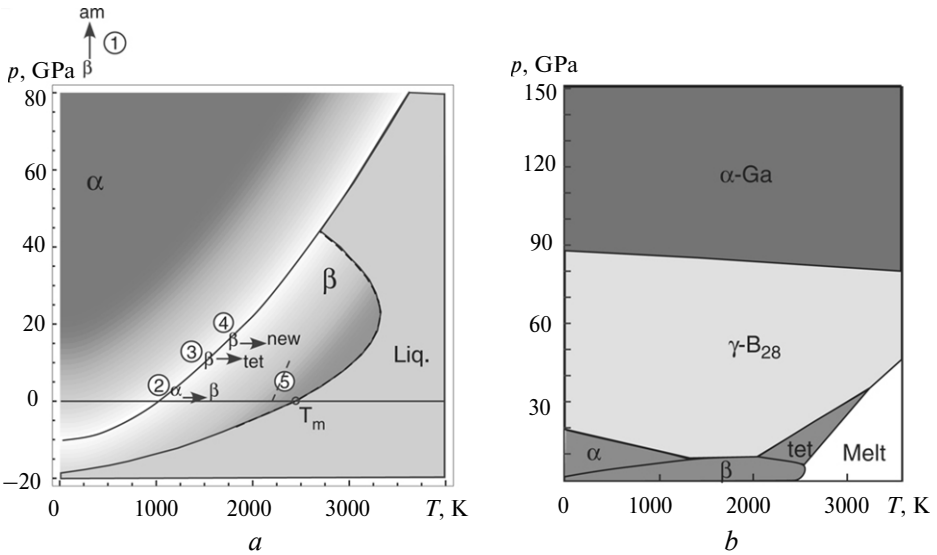

Fig. 1. Prediction of the phase diagram of boron by the present author [11] (*a*); the numbers indicated are experiments, concrete references are given in the text. Prediction by Oganov et al. [12] (*b*); for easy of comparison, the axes have been changed in order to match with the left-hand figure.

So far, only a few experimental data are available in scattered range of p, T, which are indicated by numbers in Fig. 1, *a*. Runow observed a transition from α to

β phase at an estimated temperature of 1370 °C (denoted by 2) [15]. Although the lattice spacing was perfect, there was a deficiency of 9 atoms for β-rhombohedral boron. The predicted phase boundary is close to this observation. This is the only experiment for α-rhombohedral boron as the starting material.

When β-rhombohedral boron is used as the starting material, it is transformed to an amorphous phase at $p > 100$ GPa at the ambient temperature (denoted by 1) [1]. This pressure is far higher than the predicted phase boundary. However, this does not necessarily indicate that the prediction is wrong. Remember that the room temperature is so low compared with the melting point of boron that the reaction rate is too slow to be observed. There are many examples showing that at low temperatures metastable phases survive in a wide range of pressures [16]. To that extent, the kinetics of reactions often hinders the true phase boundary. As has been shown soon later, we may interpret this amorphization at 100 GPa as indicating that β-rhombohedral boron is not stable at high pressures.

At elevated temperatures, β-rhombohedral boron is transformed to a tetragonal phase at $p > 10$ GPa (denoted by 3) [2]. The tetragonal phase is not considered in Fig. 1, *a*. However, as described previously, the density of the tetragonal phase is an intermediate between those of α- and β-rhombohedral boron (see Table 2 of the first part), so that it is reasonable to expect that the stable region of the tetragonal phase appears at the middle of those regions of α- and β-rhombohedral boron.

Recently, Mori et al. observed that at the ambient temperature α-rhombohedral boron is stable up to 200 GPa [17]. This is in contrast to the situation of β-rhombohedral boron, for which the amorphization occurs at 100 GPa. Hence, it is clear that α-phase is more stable than β-phase at high pressures. Neither the α-Ga type nor later discussed γ-phase appeared. Even though the energy minimum of the α-Ga type and γ-phase is lower than that of α-rhombohedral boron, the energy barrier for α-rhombohedral boron to have to override may be too high to reach there. On the other hand, for β-rhombohedral boron, it is certain that α-phase transition occurs, even though the phase, to which β-rhombohedral boron transforms, is not clear. This fact itself confirms our simple perspective about the stability of boron polymorphs; a denser phase is more stable than a dilute phase at high pressure [14, 18].

For the melting curve, a more recent data should be referred to [19] (denoted by 5). The discrepancy to the experiment is discussed in [20]. A note should be mentioned about the anomaly in the resistivity. Experimentalists sometimes observe step structures in the pressure dependence of the resistivity [21—23]. The step structure is frequently referred to as indicating phase transitions. However, this is not the case at least for α-rhombohedral boron. Even though there is no phase transition, a band bowing can give rise to such a discontinuity [24].

There was one concern with this phase diagram. An unknown phase denser than α-phase was once reported by Wentorf (denoted by 4) [25]. Since nothing was known about this phase except the powder X-ray diffraction pattern, we could not do anything other than leaving it alone. To our surprise, this phase has been recently identified as γ-orthorhombic boron [12, 26—28].

Then, Oganov et al. have provided an alternative and more comprehensible phase diagram, by combination of calculation and experiment [12]. This is shown in Fig. 1, *b*. As shown in Table 2 of Part 1 of this review (see Сверхтв. материалы. — 2010. — № 3. — С. 82—108; J. Superhard Materials. — 2010. — **32**, N 3. — P. 205—225), the density of γ-phase is the highest. Therefore, according to the general rule, it is reasonable that γ-phase is the most stable phase at high pressures. The tetragonal phase, which is missed in (a) is provided in (b).

Relative positions of α- and β-rhombohedral boron are the same in these two phase diagrams. A notable discrepancy is again the stability of α- and β-rhombohedral boron at $p = 0$ and $T = 0$. It should be noted that this discrepancy occurs within the energy difference about 10 meV/atom. This order of magnitude is still outside the accuracy, which the present DFT calculations (including GGA) can reach [29]. Owing to this energy uncertainty, the error bar of the calculated transition pressure will be several GPa.

An examination of the transition between α- and β-phases up to 50 GPa has been conducted by Mori et al. [30]. As usual in high-temperature experiments, reactions with unwanted parts of the apparatus sometimes take place, which makes it difficult to perform X-ray diffraction study. Historically, such unknown peaks have been sometimes recognized since Decker and Kasper reported for the first time the crystal structure for α-boron [31].

The equations of states have been examined for various polymorphs; for β-rhombohedral boron in ranges of 0—10 GPa [32], 0—100 GPa [1], and 0—30 GPa with elevated temperatures [2], for α-rhombohedral boron 0—100 GPa [17, 33], and for boron carbide 0—11 GPa [34]. In all the cases, Murnaghan's equation-of-state [35]

$$\frac{V(p)}{V_0} = \left(1 + \frac{B_1}{B_0}\right)^{-1/B_1} \tag{1}$$

is well fitted. The bulk modulus B_0 at $p = 0$ and its pressure derivative B_1 so obtained are in good agreement with the calculation. Therefore, experimentalists can readily estimate the density of boron-rich solids at high pressures from the volume at $p = 0$, irrespective the crystal structure.

Classification of phase transitions

Combining the phase diagram with knowledge of the chemical trends in the deformation potential, we are able to delineate a general trend in the electronic hardness. In Fig. 2, shown are contour maps of the deformation potential, that is, here it means the pressure dependence of the energy gap dE_g/dp, in the two-dimensional space of the coordination number (N_c) and the complexity of crystal. The qualitative terminology complexity is used to roughly mean the number of atoms in a crystal cell. For a typical tetrahedrally coordinated semiconductor, it is two or a small value. As the complexity increases, the roles of defect and entropy effect increase, and chances to encounter frustration will increase. For β-rhombohedral boron and clathrate crystals, there are a large number of atoms in the cell, and thereby large complexity.

For most of materials, dE_g/dp is negative. Tetrahedrally coordinated semiconductors are stable due to forming strong covalent bonds. The cost of it is a small coordination number. According to the classification of the crystal stability in [36], this stability belongs to the second category, that is, highly oriented covalent bonds maintain the crystal structure against shear strains. Ionic crystals such as NaCl type have larger coordination number, forming close-packed structures. In this case, the cost of possessing a large coordination number is that an individual bond is not so strong. The crystal stability belongs to the first category [36], that is, a large number of the coordination imposes constraints on the deformation for shear strains. As pressure increases, ionic crystals tend to shrink their gap rapidly, because of the weak deformation potential. Therefore, the band closure readily occurs at low pressures. Semiconductors are relatively hard

materials, so that the deformation potential is small. The band-closure pressure is expected to be high, of the order of 100 GPa. At such high pressures, a small coordination number has a disadvantage, because strong stress should be sustained by a small number of bonds. Then, a drastic change of the phase transition occurs, if an appropriate phase is available near the original phase. If there is no such phase near the original phase, or if the temperature is so low that the atomic relaxation is too slow, amorphization occurs. In fact, irreversible transformation to amorphous phases was observed in clathrate compounds: Ba_8Si_{46} (at 40 GPa) [37], K_8Si_{46} (32 GPa) [38], and $Ba_{24}Si_{100}$ (23 GPa) [39]. The amorphization of β-rhombohedral boron can be classified as this category with a higher pressure.

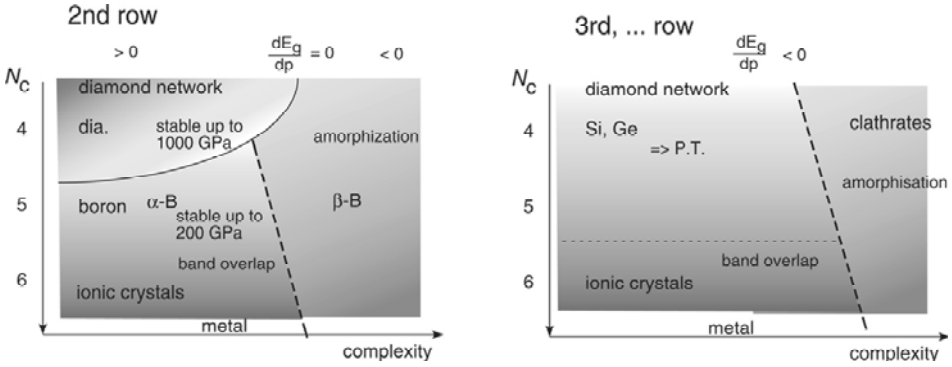

Fig. 2. Classification of phase transitions (P.T.). The figures are contour maps of the pressure dependence of the energy gap dE_g/dp in the two-dimensional space of the coordination number N_c and complexity of crystal. The line $dE_g/dp = 0$ is indicated to separate regions of positive and negative dE_g/dp. See text.

As going up from a larger row to a small row in the periodic table, the covalency increases. Hence, the deformation potential decreases toward zero, and eventually turns to positive. This happens for diamond. For diamond, the gap increases with increasing pressure. There is no phase transition up to about 1000 GPa. The boron case lies between Si and diamond: the deformation potential is an intermediate between them. However, the coordination number of boron is larger than that of Si. This is one reason why only α-rhombohedral boron undergoes gap closure without any phase transition. Another and more important reason is the geometrical effect: the icosahedron is so flexible that it allows the coordination number to change calmly [40].

Many phase transitions of insulators can be qualitatively classified in this scheme. Recent discovery of the transformation of metal sodium to an insulating phase at a high pressure is a surprising matter [41]. This case is out of the present scheme. From very beginning, metal Na has a large number of coordination, i.e. 8 for a bcc structure. At very high pressures, atoms are so close, even core electrons are overlapped. Too accumulation of electrons at the nearest-neighbouring region results in mutual repulsion of electrons. Then, valence electrons are squeezed to the second-nearest neighbouring region. The second-nearest neighbouring region is 6-fold in bcc, which is a driving force to cause the phase transition.

Future development in the material research. In closing this section, I like to mention a personal perspective for the material research around boron. In a binary B—C system, only boron carbide is a stable phase [42, 43]. Despite, we have seen successive discoveries of new superhard materials, such as BC_5 and γ-

orthorhombic boron [44]. Further survey has been progressed in various ways, for example, a theoretical study in the B_nC_m system [45]. Even in well-studied graphite, a new phase with monoclinic structure was found [46]. Among nanostructure materials, new phases have been discovered, such as boron nanowires [47], nanobelts [48], and nanoribbons [49]. The success of synthesizing BC_5 by Solozhenko et al. shows that even unstable compounds, which do not appear in the phase diagram, can be synthesized under special circumstances [50]. They chose a mixture of BC_3 and graphite as the starting material, where graphite-like BC_3 itself is very scarcely obtained [51, 52]. In this way, there will still be many chances to find unseen superhard materials, when special conditions are prepared.

In the material research, one mission of theory is the calculation of phase diagrams, from which experimentalists can get useful ideas. For heavily B-doped diamond, Ekimov et al. used high-pressure method [53]. In analyzing the reaction of their method, $B_4C + G \rightarrow B@D$ (G and D are denoted as graphite and diamond, respectively), it is suggested that high concentrations of B-doped diamond can be synthesized by using high pressure [54]. A similar consideration leads us to find appropriate conditions for preparation of BC_5 [55]. Another mission of the theory is a structural prediction at arbitrary conditions [56—58]. In particular, a sophisticated algorithm, such as evolutionary algorithm [58] is a powerful tool, as evident in the discovery of γ-orthorhombic boron.

MECHANICAL PROPERTIES

Elastic constants

Let us discuss mechanical properties of boron and boron-rich solids. In Table 1, bulk modulus and elastic constants are compared among α-, β-rhombohedral boron, and boron carbide. For the boron carbide case, the elastic constant is not so much sensitive to the composition. By viewing from the bulk modulus, we see that β-rhombohedral boron is the softest polymorph among the boron solids. Boron carbide is on the contrary the hardest one.

Table 1. Bulk modulus, its pressure derivative, elastic constants of α- and β-rhombohedral boron and boron carbide. The data without a reference are taken from [14]

Polymorph	α-rhombohedral		β-rhombohedral		boron carbide	
	experiment	calculation	experiment	calculation	experiment	calculation
B, GPa	213—224[a]	218.4	185—210[b]	203.5	234.9[c] 199[d]	245.5[c]
dB/dp	4.0	4.8	2.2, 4.2	4.5		4.95
θ_D, K	1430[f]		1200—1300[g]			
C_{ij}, GPa		[h]	[i]			[j]
11		464.2	467			500.4
33		628.4	473			430.2
44		205.0	198			
12		133.3	241			125.3
13		38.5	—			73.9
14		–19.0	15.1			7.7

Notes: [a][32]; [b][1]; [c][59]; [d][34]; [e][60]; [f][61]; [g][62]; [h][63]; [i][64]; [j][65].

As a whole, the magnitude of elastic constants also accords to this order. However, some comments on the individual component should be mentioned. The first is C_{44} component of α-rhombohedral boron. A study using force constant model shows that C_{44} component would vanish, if angle bending forces are ignored; see Table 1 of [36] and Table 2 of [63]. Actually, C_{44} component is not small, but rather large as compared with β-rhombohedral boron. This infers that the mechanical stability of α-rhombohedral boron is maintained by the angle forces. The angle force is a characteristic of the covalent bond, from which the covalent character of the *inter*icosahedral bond is evident, as discussed in Part 1 of the review (Section "Significance of angle bending forces").

The second is the effect of atom relaxation. *The internal response of crystal is not always similar to the externally applied strain*, because of the internal relaxation. The elastic constants $C_{\mu\alpha\nu\beta}$ are expressed by

$$C_{\mu\alpha\nu\beta} = \{\mu\alpha, \nu\beta\} + (\mu\alpha, \nu\beta), \quad (2)$$

according to the notations of Born and Huang [66]. The first term of the right-hand side $\{\mu\alpha, \nu\beta\} \equiv \hat{\hat{C}}_{\mu\alpha\nu\beta}$ represents the contribution of homogeneous deformation and the second term $(\mu\alpha, \nu\beta)$ represents the so-called internal shift, which is the atom relaxation induced by the external strain. Usually, the first term is the most important, but the second term sometimes plays an essential role as well. The internal shift is represented by the optical phonons induced by the external strain. When a low-frequency mode is involved in the induced phonons, the effect of this internal shift becomes significant [36]. Without taking this effect into account, flat interpretation is risky, in particular, for flexible icosahedron-based boron crystals [2]. Graphical illustration of the internal shift caused by a strain confirms us how efficiently the librational mode of α-rhombohedral boron and boron carbide can release the external strain [67].

A good example for the effect of relaxation is seen in comparison between C_{11} and C_{33} components. When we look at the structure of boron-rich solids, as shown in Fig. 1 of the first part of the review, our intuitive expectation for the elastic constants is that the crystal is more stiff in the c-axis than in *ab*-plane, i.e., $C_{11} < C_{33}$. This is because the strongest *inter*icosahedral bonds are more inclined to the *c*-axis. This is actually the case for α-rhombohedral boron, as shown in Table 1. However, for boron carbide, even the strongest C chain is inserted along the *c*-axis, the insertion does not enhance at all the stiffness along this axis. Surprisingly, the opposite result is obtained, i.e., $C_{11} > C_{33}$. Lee et al. obtained this relationship numerically, but nothing is stated about the mechanism. Even obtaining the correct answer by first-principles calculations, interpreting the result is not easy. The reason is a slight deflection of the apex angle αrh of the rhombohedral lattice from 60° [36]. As later shown, a slight deviation from 60° has the decisive role of the way of atom relaxation. Even though stiff bonds are aligned almost along the *c*-axis, deformable icosahedra enable the internal shift so effectively. The analogy of magic hand helps our understanding of this effect [68].

Volume compressibility

There are criticisms for the traditional understanding that *inter*icosahedral bond is stronger than *intra*icosahedral bond. However, the evidence of these criticisms seems the volume compressibility only [69, 70]. I like to stress that which way we evaluate the stiffness must be declared whenever we refer to stiffness, otherwise the argument would result in cross-purposes. In the following, I show how such

apparent contradictions are resolved without introducing any exotic mechanism [18, 71].

First, let us consider how the relaxation occurs for hydrostatic pressure. The pressure derivatives of various structural parameters ξ are compared with the deviation of the apex angle from 60° (FCC), Δαrh, in Table 2. One can see that the initial change in the apex angle α_{rh} is such a manner that the deviation $\Delta\alpha_{rh}$ is increased: the negative value of $\Delta\alpha_{rh}$ for α-rhombohedral boron becomes more negative, and the positive value of $\Delta\alpha_{rh}$ for β-rhombohedral boron or boron carbide more positive. In other words, the anisotropy of the crystal increases for all the cases. Caution is needed for the experimental value $\partial\ln\alpha_{rh}/\partial p$ for β-rhombohedral boron. The listed data is obtained by Ma et al., which clearly resolved the pressure dependence of ahex and chex [2]. This gives a positive value for $\partial\ln\alpha_{rh}/\partial p$. On the other hand, those data of [32] and [1] seem to give negative values for $\partial\ln\alpha_{rh}/\partial p$. In these data, the pressure dependence of ahex and chex is so close, that it is marginal to resolve which is larger. Hence, we can ignore those data of [32] and [1] for the argument on $\Delta\alpha_{rh}$. In this way, we have seen that the way of deformation, which enhances the initial anisotropy of crystal is the way in which the relaxation is most efficient.

Table 2. Compressibility of various internal coordinates (ξ) of α-, β-boron, and boron carbide (B_4C) at $p = 0$. Only the first row of data is different from compressibility, but the deviation of the angle arh from 60°. The compressibility k is defined as $k = \partial\ln\xi/\partial p$ and is given in TPa^{-1}. For β-rhombohedral boron, only the icosahedron at the corner of the rhombohedron is shown. All the data without the reference are the author's calculation

	ξ	α-rhombohedral	β-rhombohedral	boron carbide
$\Delta\alpha_{rh}$, deg		–1.35[a]	+5.22[a]	+6.40[a]
cell	α_{rh}	–0.11	+0.14[a]	+0.20[a]
	α_{rh}	–1.11	–1.50[b]	–1.16[a]
			–1.80[c]	
	V_{cell}	–4.06		
		–4.14[b]	–4.46[b]	
		–4.50[d]	–5.30[c]	–4.03[d]
		–4.20[e]		–4.90[f]
inter-	r_2	–1.66		
	r_3	–1.35		
intra-	h	–1.31	–1.00[b]	–0.96[a]
	w	–0.89	–1.50[b]	–1.20[a]
	V_{ico}	–3.09		–3.64[a]
		–3.36[d]		–6.20[f]
chain			–2.70[b]	–0.60[a]

Notes: [a][18]; [b][14]; [c][2]; [d][70]; [e][32]; [f][34].

Let us look at the compressibility, $\kappa_\xi = \partial\ln\xi/\partial p$, for an internal parameter ξ. In almost all the cases listed, the volume compressibility of the icosahedron is smaller in the magnitude than that of the unit cell,

$$|\kappa_{V\text{ico}}| < |\kappa_{V\text{cell}}|. \quad (3)$$

This relationship can be alternatively seen by comparing the compressibility of $\xi = r_2$ with the averaging compressibility of $\xi = h$ and $\xi = w$. The exception is an experiment by Nelmes et al. [34], to which Lazzari et al. shed a suspicious. For the moment, we will ignore this exception. The observation of the small compressibility of the icosahedra seems to be the primary reason for the strong *intra*icosahedral bonding in these papers [69, 70].

This apparent contradiction of the volume compressibilities with the traditional understanding is easily solved [18, 71]. Even though the strengths of individual bonds follow Eq. (2) of Part 1, don't miss that there is yet another contribution to the compressibilities. The number of *intra*icosahedral bonds N_{in} is 10 times larger than that of the two-center *inter*icosahedral bonds N_2. Under hydrostatic pressures, all the bonds equally work on the deformation. This gives a balance in the restoring forces for a uniform deformation, as

$$N_{in}f_{in} : N_2f_2 = 10 : 3. \quad (4)$$

This says that the icosahedron is more rigid. The situation is very like the situation of a balloon: if one tries to compress even a soft balloon uniformly, one feels a large restoring force and the balloon appears stiff.

Volume rigidity does not necessarily imply rigidity against any deformation. Rather the icosahedron of boron crystals is more deformable like a balloon. Let us next check the deformation of the icosahedra. Compare the relative changes between the height h and the width w of the icosahedron in Table 2. Interestingly, for α-rhombohedral boron, the icosahedron is flattened in the ab plane, while the cell is elongated along the c axis. The opposite response occurs in B_4C and β-rhombohedral boron. These deformations are schematically illustrated in Fig. 3.

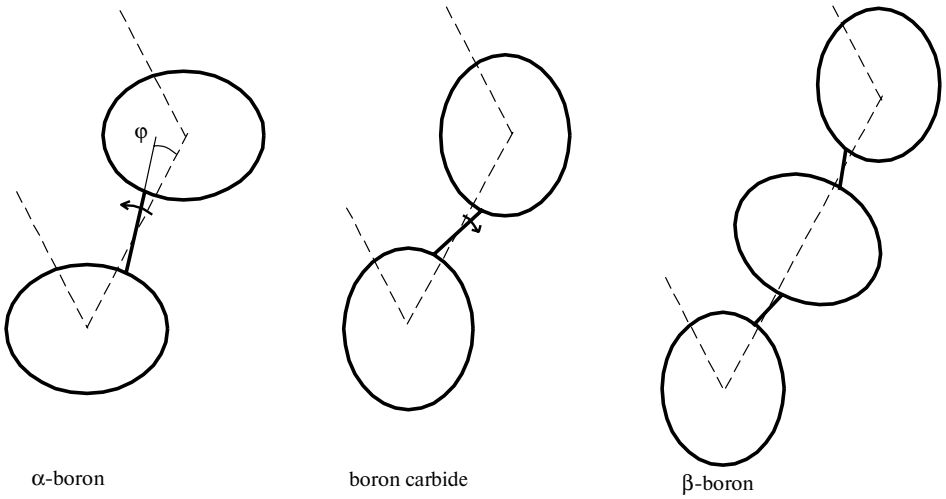

Fig. 3. Deformation of icosahedra of α-, β-rhombohedral boron, and boron carbide under hydrostatic pressure. Note that the *inter*icosahedral bond is deflected from the lattice vector by angle φ.

To understand this response, the fact of the deflection of the *inter*icosahedral bond from the lattice vector, φ, is crucial. The readers may notice that the sign of φ is correlated to the sign of $\Delta\alpha_{rh}$. In all the cases, the deflection of the *inter*icosahedral bond from the lattice vector increases with increasing pressure. This way is the way in which the increase in the elastic energy of the *inter*icosahedral bond is suppressed. This indicates that the deformation of the *inter*icosahedral bond has the highest priority in determining the strain energy. If

the *intra*icosahedral bond were stronger than the *inter*icosahedral bond, the icosahedron would deform uniformly and φ would either change in opposite direction or not change. The same argument naturally leads to the reason why the crystal of α-rhombohedral boron has nonzero φ from beginning. For more details, see Appendix of [40].

In this way, in all the above high-pressure experiments, I find no strange response, which is in conflict with the traditional understanding.

ACKNOWLEDGMENTS

This work was partly supported by a Grant-in-Aid for Scientific Research in Priority Areas "Areas of New Materials Science Using Regulated Nano Spaces" (No. 20045009) from MEXT, Japan.

У другій частині огляду розглянуто фазову діаграму бору. Порівняно фазову стабільність кристалів і зроблено спробу вивести загальні тенденції, які б дозволили отримати уявлення про майбутнє надтвердих матеріалів. Розглянуто механічні властивості бору і кристалів з високим вмістом бору як основи надтвердих матеріалів. Ця область є головним джерелом багатьох суперечностей стосовно сильного міжікосаедричного зв'язку. На основі вивчення багаточисельних прикладів деформації дано логічні трактовки зв'язку.

***Ключові слова**: кристали з високим змістом бору, розрахунки з перших принципів, фазовий перехід, механічні властивості.*

Во второй части обзора рассматрена фазовая диаграмма бора. Сравнена фазовая стабильность кристаллов и сделана попытка вывести общие тенденции, которые позволили бы получить представление о будущем сверхтвердых материалов. Рассмотрены механические свойства бора и кристаллов с высоким содержанием бора как основы сверхтвердых материалов. Эта область исследований является основным источником многих разногласий относительно прочной межикосаэдрической связи. На основании изучения многочисленных примеров деформации даны логические трактовки связи.

***Ключевые слова**: кристаллы с высоким содержанием бора, расчеты из первых принципов, фазовый переход, механические свойства.*

1. *Sanz D. N., Loubeyre P., Mezouar M.* Equation of state and pressure induced amorphization of β-boron from X-ray measurements up to 100 GPa // Phys. Rev. Lett. — 2002. — **89**. — P. 245501 (4 p.).
2. *Ma Y., Prewitt C. T., Zou G. et al.* High-pressure high-temperature X-ray diffraction of β-boron to 30 GPa // Phys. Rev. B. — 2003. — **67**. — P. 174116—174121.
3. *Haüssermann U., Simak S. I., Ahuja R., Johansson B.* Metal-nonmetal transition in the boron group elements // Phys. Rev. Lett. — 2003. — **90**. — P. 065701 (4 p.).
4. *Zhu W.-J., Henley C. L.* Effective potentials for 6-coordinated boron: structural geometry approach // Europhys. Lett. — 2000. — **51**. — P. 133—139.
5. *Segall D. E., Arias T. A.* Ab initio approach for high-pressure systems with application to high-presure phases of boron: Perturbative momentum-space potential // Phys. Rev. B. — 2003. — **67**. — P. 064105 (15 p.).
6. Golikova O. A. Electrocal properties of α-rhombohedral boron // Sov. Phys. Semicond. — 1979. — **13**. — P. 486—487.
7. *Hoard J. L., Hughes R. E.* Elemental boron and compounds of high boron content: Structure, properties, and polymorphism // The chemistry of boron and its compounds / Ed. by E. L. Muetterties. — New York: John Wiley, 1967. — Chap. 2.
8. *Soga K., Oguri A., Araake S. et al.* Li- and Mg-doping into icosahedral boron crystals, α- and β-rhombohedral boron, targeting high-temperature superconductivity: Structure and electronic states // J. Solid State Chem. — 2004. — **177**. — P. 498—506.
9. *Horn F. H.* On the crystallization of simple rhombohedral boron from platinum // J. Electrochem. Soc. — 1959. — **106**. — P. 905—906.
10. *Tallant D. R., Aselage T. L., Campbell A. N., Emin D.* Boron carbide structure by raman spectroscopy // Phys. Rev. B. — 1989. — **40**. — P. 5649—5656.

11. *Shirai K., Masago A., Katayama-Yoshida H.* High-pressure properties and phase diagram of boron // Phys. Status Solidi B. — 2007. — **244**. — P. 303—308.
12. *Oganov A. R., Chen J., Gatti C. et al.* Ionic high-pressure form of elemental boron // Nature. — 2009. — **457**. — P. 863—867.
13. *Mailhiot C., Grant J. B., McMahan A. K.* High-pressure metallic phases of boron // Phys. Rev. B. — 1990. — **42**. — P. 9033—9039.
14. *Masago A., Shirai K., Katayama-Yoshida H.* Crystal stabilities of α- and β-borons // Ibid. — 2006. — **73**. — P. 104102—104111.
15. *Runow P.* Study of the α to β transformation in boron // J. Mater. Sci. — 1972. — 7. — P. 499—511.
16. *According* to the phase diagram of carbon (for example: *Bundy F. P., Bassett W. A., Weathers M. S. et al.* The pressure-temperature phase and transformation diagram for carbon // Carbon. — 1996. — **34**. — P. 141—153), diamond should not exist at room temperature. On the other hand, graphite could not exist at high pressures more than 2 GPa. However, experiments at room temperature show the presence of graphite up to around 10 GPa. See for example: *Yagi T., Utsumi W., Yamakata M. et al.* High-Pressure in situ X-ray-diffraction study of the phase transformation from graphite to hexagonal diamond at room temperature // Phys. Rev. B. — 1992. — **46**. —P. 6031—6039; *Miller E. D., Nesting D. C., Badding J. V.* Quenchable transparent phase of carbon // Chem. Mater. — 1997. — **9**. — P. 18—22.
17. *Mori Y., Fujii Y., Hyodo H. et al.* X-Ray diffraction study of α-boron up to 200 GPa // 13th Int. Conf. High Pressure Semiconductor Physics. — Fortaleza, Brazil, 2008.
18. *Shirai K., Masago A., Katayama-Yoshida H.* High-pressure properties of icosahedron-based solid borons // Phys. Status Solidi B. — 2004. — **241**. — P. 3161—3167.
19. *Brazhkin V. V., Taniguchi T., Akaishi M., Popova S. V.* Fabrication of β-boron by chemical-reaction and melt-quenching methods at high pressures // J. Mater. Res. — 2004. — **19**. — P. 1643—1648.
20. *Shirai K., Dekura H., Masago A.* Superconductivity research on boron solids and an efficient doping method // J. Phys.: Conf. Ser. — 2009. — **176**. — P. 012001—012018.
21. *Eremets M. I., Struzhkin V. V., Mao H., Hemley R. J.* Superconductivity in boron // Science. — 2001. — **293**. — P. 272—274.
22. *Kaneshige M., Shimizu K., Hyodo H., Kimura K.* Measurement of the electrical resistance in α-boron under high pressure // 48th High-Pressure Conf. of Japan. — Kurayoshi, Japan: Jpn. Soc. High Pressure Sci. Technol., 2007. — 1C06.
23. *Shimizu K., Kaneshige M., Hashimoto Y. et al.* Superconductivity in α-boron at Mbar pressure // Physica C. — Available online 13 November 2009.
24. *Shirai K., Dekura H., Yanase A.* Electronic structure and electrical resistivity of α-boron under high pressure // J. Phys. Soc. Jpn. — 2009. — **78**. — P. 094714—094723.
25. *Wentorf R. H.* Jr. Boron: another form // Science. — 1965. — **147**. — P. 49—50.
26. *Solozhenko V. L., Kurakevych O. O., Oganov A. R.* On the hardness of a new boron phase, orthorhombic γ-B_{28} // J. Superhard Materials. — 2008. — **30**. — P. 428—429.
27. *Zarechnaya E. Y., Dubrovinsky L., Dubrovinskaia N. et al.* Synthesis of an orthorhombic high pressure boron phase // Sci. Tech. Advanced Materials. — 2009. — **9**. — P. 044209 (4 p.).
28. *Zarechnaya E. Y., Dubrovinsky L., Dubrovinskaia N. et al.* Superhard semiconducting optically transparent high pressure phase of boron // Phys. Rev. Lett. — 2009. — **102**. — P. 185501 (4 p.).
29. *The phase* stability within energy difference of 10 meV/atom holds for diamond-graphite or cubic-hexagonal BN systems: *Shirai K., Fujita H., Katayama-Yoshida H.* Pressure-induced phase transitions of BNs // Phys. Status Solidi B. — 2003. — **235**. — P. 526—530. Further references are therein. Even for these familiar systems, the accuracy of the present DFT calculations is not enough to answer which structure is stable.
30. *Fujii T., Fujii Y., Fujii A. et al.* Possibility of the synthesis of α-boron under high pressure and temperature // Fall Meeting of the Physical Society of Japan, Iwate, 2008. — 22pWF-11.
31. *Decker B. F., Kasper J. S.* The crystal structure of a simple rhombohedral form of boron // Acta Cryst. — 1959. — **12**. — P. 503—506.
32. *Nelmes R. J., Loveday J. S., Allan D. R. et al.* Neutron and X-ray-diffraction measurements of the bulk modulus of boron // Phys. Rev. B. — 1993. — **47**. — P. 7668—7673.
33. *Polian A., Chervin J. C., Munsch P,* Gauthier M. α-boron at very high pressure: structural and vibrational properties // J. Phys.: Conf. Ser. — 2008. — **121**. — P. 042017—042020.

34. *Nelmes R. J., Loveday J. S., Wilson R. M. et al.* Observation of inverted-molecular compression in boron carbide // Phys. Rev. Lett. — 1995. — **74**. — P. 2268—2271.
35. *Murnaghan F. D*. The compressibility of media under extreme pressures // Proc. Natl. Acad. Sci. U.S.A. — 1944. — **30**. — P. 244—247.
36. *Shirai K.* The elastic properties and the mechanical stability of icosahedral boron crystals // Phys. Rev. B. — 1997. — **55**. — P. 12235—12243.
37. *Miguel A. S., Merlen A., Toulemonde P. et al.* Pressure-induced homothetic volume collapse in silicon clathrates // Europhys. Lett. — 2005. — **69**. — P. 556—562.
38. *Tse J. S., Desgreniers S., Li Z.-q. et al.* Structural stability and phase transitions in K_8Si_{46} clathrate under high pressure // Phys. Rev. Lett. — 2002. — **89**. — P. 195507 (4 p.).
39. *Shimizu H., Kume T., Kuroda T. et al.* High-pressure raman study of he ba-doped silicon clathrate $Ba_{24}Si_{100}$ up to 27 GPa // Phys. Rev. B. — 2005. — **71**. — P. 094108 (5 p.).
40. *Shirai K., Dekura H., Mori Y. et al.* Structural study of α-boron at high pressure // Submitted to Phys. Rev. B.
41. *Ma Y., Eremets M., Oganov A. R. et al.* Transparent dense sodium // Nature. — 2009. — **458**. — P. 182—185.
42. *Bouchacourt M., Thevenot F.* Études sur le carbure de bore III. Momaine d'existence de la phase carbure de bore // J. Less-Common Metals. — 1978. — **59**. — P. 139—152.
43. *Beauvy M.* Stoichiometric limits of carbon-rich boron carbide phases // J. Less-Common Metals. — 1983. — **90**. — P. 169—175.
44. *Currently*, the structure of BC_5 is being debated. See for example, *Calandra M., Mauri F.* High-T_c superconductivity in superhard diamondlike BC_5 // Phys. Rev. Lett. — 2008. — **101**. —P. 016401 (4 p.); *Yao Y., Tse J. S., Klug D. D.* Crystal and electronic structure of superhard BC_5: first-principles structural optimizations // Phys. Rev. B. — 2009. — **80**. — P. 094106 (6 p.); *Jiang C., Lin Z., Zhao Y.* Superhard diamondlike BC_5: a first-principles investigation // Ibid. — 2009. — **80**. — P. 184101 (6 p.); *Liang Y., Zhang W., Zhao J., Chen L.* Superhardness, stability, and metallicity of diamondlike BC_5: density functional calculations // Ibid. — 2009. — **80**. — P. 113401 (4 p.).
45. *Kobayashi K., Arai M., Yamamoto K.* First-principles study of C_6B_2 and related compounds // Sci. Tech. Advanced Materials. — 2006. — **7**. — P. S71—S77.
46. *Li Q., Ma Y., Oganov A. R. et al.* Superhard monoclinic polymorph of carbon // Phys. Rev. Lett. — 2009. — **102**. — P. 175506 (4 p.).
47. *Zhang Y., Ago H., Ohshima M. Y. T. K. S. et al.* Synthesis of crystalline boron nanowires by laser ablation // Chem. Comm. — 2002. — **23**. — P. 2806—2807.
48. *Wang Z., Shimizu Y., Sasaki T. et al.* Catalyst-free fabrication of single crystalline boron nanobelts by laser ablation // Chem. Phys. Lett. — 2003. — **368**. — P. 663—667.
49. *Xu T. T., Zheng J. G., Nicholls A. W. et al.* Crystalline boron nanoribbons: synthesis and characterization // Nano Lett. — 2004. — **4**. — P. 963 — 968.
50. *Solozhenko V. L., Kurakevych O. O., Andrault D. Y. et al.* Ultimate metastable solubility of boron in diamond: synthesis of superhard diamondlike BC_5 // Phys. Rev. Lett. — 2009. — **102**. — P. 015506 (4 p.), (Erratum) 2009. — **102**. — P. 179901 (1 p.).
51. *Kouvetakis J., R. Kaner B., Sattler M. L., Barlett N.* A novel graphite-like material of composition BC_3, and nitrogen-carbon graphites // J. Chem. Soc. Chem. Commun. — 1986. — N 24. — P. 1758—1759.
52. *Yanagisawa H., Tanaka T., Ishida Y. et al.* Phonon dispersion curves of a BC_3 honeycomb epitaxial sheet // Phys. Rev. Lett. — 2004. — **93**. — P. 177003 (4 p.).
53. *Ekimov E. A., Sidorov V. A., Bauer E. D. et al.* Superconductivity in diamond // Nature. — 2004. — **428**. — P. 542—545.
54. *Shirai K., Dekura H., Yanase A.* Utilization of high pressure for synthesizing superconducting semiconductors: analysis of Ekimov's method // Phys. Status Solidi B. — 2009. — **246**. — P. 673—678.
55. *Nakae N., Ishisada J., Dekura H., Shirai K.* Theoretical investigation on synthesizing BC_5 crystal // J. Phys.: Conf. Ser. — 2010. — **215**. — P. 012116 (7 p).
56. *Martonrak R., Laio A., Parrinello M.* Predicting crystal structures: the parrinello-rahman method revisited // Phys. Rev. Lett. — 2003. — **90**. — P. 075503 (4 p.).
57. *Pickard C. J. Needs R. J.* High-pressure phases of silane // Ibid. — 2006. — **97**. — P. 045504 (4 p.).
58. *Oganov A. R., Glass C. W.* Crystal Structure prediction using ab initio evolutionary techniques: principles and applications // J. Chem. Phys. — 2006. — 124. — P. 244704 (15 p.).

59. *Manghnani M. H., Wang Y., Li F. et al.* Elastic and vibrational properties of B_4C to 21 GPa // Proc. Int. Conf. High Pressure Science and Technology (AIRAPT-17). — Hawaii, 1999. — P. 945—948.
60. *Shirai K., Katayama-Yoshida H.* Crystal stability of boron carbide B_{12}(CBC) // Proc. 25th Int. Conf. Phys. Semicond. — Springer, Osaka, 2000. — P. 1673—1674.
61. *Slack G. A., Oliver D. W., Horn F. H.* Thermal conductivity of boron and some boron compounds // Phys. Rev. B. — 1971. — **4**. — P. 1714— 1720.
62. *Slack G. A.* Thermal conductivity of elements with complex lattices: B, P, S // Phys. Rev. — 1965. — **139**. — P. A507—515.
63. *Shirai K., Katayama-Yoshida H.* The narrow raman linewidth of a librational mode of α-rhombohedral boron and its anharmonic effects // J. Phys. Soc. Jpn. — 1998. — **67**. — P. 3801—3808.
64. *Silvestrova I. M., Belayev L. M., Pisarevski Y. V., Niemyski T.* Acoustic properties of β-rhombohedral boron // Mater. Res. Bull. — 1974. — **9**. — P. 1101—1106.
65. *Lee S., D Bylander. M., Kleinman L.* Computational search for the real tetragonal B_{50} // Phys. Rev. B. — 1992. — **45**. — P. 3245—3251.
66. *Born M., Huang K.* Dynamical theory of crystal lattices. — Oxford: Oxford University Press, 1954. — 420 p.
67. *Shirai K.* Rotation-induced relaxation mechanism: application to boron-rich crystals // J. Solid State Chem. — 1997. — **133**. — P. 322—326.
68. *Shirai K.* Central and non-central forces on the lattice dynamics of boron-rich solids: bonding nature of icosahedral boron solids // Ibid. — 1997. — **133**. — P. 215—223.
69. *Vast V., Baroni S., Zerah G. et al*. Lattice dynamics of icosahedral α-boron under pressure // Phys. Rev. Lett. — 1997. — **78**. — P. 693—696.
70. *Lazzari R., Vast V., Besson J. M. et al.* Atomic structure and vibrational properties of icosahedral B_4C boron carbide // Ibid. — 1999. — **83**. — P. 3230—3233; (Erratum) — 2000. — **85**. — P. 4194.
71. *Shirai K., Katayama-Yoshida H.* Effects of the geometries of boron-rich crystals on the lattice dynamics // J. Solid State Chem. — 2000. — **154**. — P. 20—25.

Nanoscience and Nanotechnology Center,
ISIR, Osaka University,

Received 28.01.10